Evidence for association of $GABA_B$ receptors with Kir3 channels and regulators of G protein signalling (RGS4) proteins

Catherine E. Fowler[1], Prafulla Aryal[1,2], Ka Fai Suen[1] and Paul A. Slesinger[1,2]

[1]*Peptide Biology Laboratory, The Salk Institute for Biological Studies, La Jolla, CA, USA*
[2]*Departments of Neurosciences and Biology, University of California, La Jolla, CA, USA*

Many neurotransmitters and hormones signal by stimulating G protein-coupled neurotransmitter receptors (GPCRs), which activate G proteins and their downstream effectors. Whether these signalling proteins diffuse freely within the plasma membrane is not well understood. Recent studies have suggested that direct protein–protein interactions exist between GPCRs, G proteins and G protein-gated inwardly rectifying potassium (GIRK or Kir3) channels. Here, we used fluorescence resonance energy transfer (FRET) combined with total internal reflection fluorescence microscopy to investigate whether proteins within this signalling pathway move within 100 Å of each other in the plasma membrane of living cells. $GABA_B$ R1 and R2 receptors, Kir3 channels, Gαo subunits and regulators of G protein signalling (RGS4) proteins were each fused to cyan fluorescent protein (CFP) or yellow fluorescent protein (YFP) and first assessed for functional expression in HEK293 cells. The presence of the fluorophore did not significantly alter the signalling properties of these proteins. Possible FRET was then investigated for different protein pair combinations. As a positive control, FRET was measured between tagged $GABA_B$ R1 and R2 subunits ($\sim$12% FRET), which are known to form heterodimers. We measured significant FRET between tagged RGS4 and $GABA_B$ R1 or R2 subunits ($\sim$13% FRET), and between Gαo and $GABA_B$ R1 or R2 subunits ($\sim$10% FRET). Surprisingly, FRET also occurred between tagged Kir3.2a/Kir3.4 channels and $GABA_B$ R1 or R2 subunits ($\sim$10% FRET). FRET was not detected between Kir3.2a and RGS4 nor between Kir3.2a and Gαo. These data are discussed in terms of a model in which $GABA_B$ receptors, G proteins, RGS4 proteins and Kir3 channels are closely associated in a signalling complex.

(Resubmitted 19 October 2006; accepted after revision 14 December 2006; first published online 21 December 2006)
Corresponding author P. A. Slesinger: The Salk Institute, 10010 North Torrey Pines Rd, La Jolla, CA 92037, USA. Email: slesinger@salk.edu

G protein-gated inwardly rectifying potassium (GIRK or Kir3) channel activity is important for regulating excitability in the heart and brain (Stanfield *et al.* 2002). Kir3 channels are activated following stimulation of G protein-coupled receptors (GPCRs) that use the Gi/o family of G proteins. Stimulation of the GPCR promotes exchange of GDP for GTP on the Gα subunit which, in turn, leads to activation of the Gα subunit and the G$\beta\gamma$ dimer. G$\beta\gamma$ dimers bind to and activate Kir3 channels (Reuveny *et al.* 1994; Wickman *et al.* 1994; Huang *et al.* 1995). Gα subunits are required for terminating Kir3 activation. The intrinsic GTPase activity of the Gα subunit hydrolyses GTP, leading to inactivation of the G$\beta\gamma$ dimer. Regulator of G protein signalling (RGS) proteins accelerate the GTPase activity of Gα subunits (GAP), leading to faster activation and deactivation of Kir3 channels (Doupnik *et al.* 1997).

Several studies suggest that the receptors, G proteins and channels may exist in a signalling complex (Lavine *et al.* 2002; Peleg *et al.* 2002; Clancy *et al.* 2005). We have recently found that the pertussis toxin (Ptx)-sensitive G$\alpha\beta\gamma$ heterotrimer (i.e. Gαi/o family) associates directly with Kir3 but not with G protein-insensitive inward rectifiers (Clancy *et al.* 2005). Mutations in the C-terminal domain of Kir3 that disrupt this interaction also impair channel activation by GPCRs (Clancy *et al.* 2005). These experiments indicate that a close association between the G protein and channel is required for efficient activation, suggesting that Kir3 channels exist in a specific signalling complex. One prediction of this hypothesis is that diffusion of proteins within the complex will be restricted. Experiments examining the lateral mobility of G proteins indicate that G proteins in the plasma membrane are constrained in their movement (Kwon

 DOI: 10.1113/jphysiol.2006.123216

et al. 1994). The protein–protein interaction of both the Gα and G$\beta\gamma$ subunits with Kir3 channels and GPCRs suggests that the Gα subunit may not dissociate from the G$\beta\gamma$ dimer upon G protein activation (Clancy *et al.* 2005). Although there is biochemical evidence for Gαq and Gαs dissociation from G$\beta\gamma$, the evidence demonstrating dissociation for Gαi/o G proteins is less clear (Rebois *et al.* 1997). Klein *et al.* (2000) demonstrated that dissociation is not a prerequisite for signalling. Directly fusing Gα to G$\beta\gamma$, thereby preventing dissociation, does not alter the signalling properties in yeast. Consistent with this finding, Bunemann *et al.* 2003) used fluorescence resonance energy transfer (FRET) to demonstrate that Gαi and G$\beta\gamma$ undergo a conformational rearrangement, rather than dissociation, during activation. Recent FRET studies have also suggested that some GPCRs are precoupled with the G protein (Gales *et al.* 2005; Nobles *et al.* 2005; but see Hein *et al.* 2005). These studies suggest that a signalling complex may exist that contains the receptor, G protein and channel.

In support of this model, Lachance *et al.* (1999) demonstrated that G$\beta\gamma$ remains associated with β2-adrenergic receptors following activation. Furthermore, Lavine *et al.* (2002) discovered that D2/D4 dopamine receptors form stable, G$\beta\gamma$-dependent complexes with Kir3 channels. The lipid environment may further segregate specific signalling molecules. For example, Kir3 channels, GABA$_B$ receptors and Gαi/o G proteins associate with lipid rafts, whereas metabotropic glutamate receptors and Gαq G proteins associate with caveolin (Becher *et al.* 2001; Oh & Schnitzer, 2001; Koyrakh *et al.* 2005). Finally, recent studies have shown that RGS proteins may stably interact with Gα G proteins (Benians *et al.* 2005) and μ opioid receptors (Georgoussi *et al.* 2006). Taken together, these studies suggest that Kir3 channels, G proteins, GPCRs, other signalling proteins (e.g. RGS proteins and receptor kinases), lipids and cytoskeletal anchoring proteins (Bloch *et al.* 2001) coexist in a macromolecular signalling complex.

We hypothesized that the G$\alpha\beta\gamma$ heterotrimer interacts with the GPCR, RGS and Kir3 proteins under resting conditions. Upon receptor activation, the Gα subunit undergoes a conformational rearrangement that reveals a surface of G$\beta\gamma$ that binds to and activates Kir3 channels (Bunemann *et al.* 2003; Clancy *et al.* 2005). Here, we asked whether these protein–protein interactions could be studied using advanced microscopic techniques. We used FRET to study these potential protein–protein interactions in living cells. The magnitude of FRET is inversely proportional to the sixth power of distance, making FRET a highly sensitive tool for detecting distances of less than 100 Å between fluorophores (Jares-Erijman & Jovin, 2003). We used total internal reflection fluorescence (TIRF) microscopy to selectively measure the FRET in the plasma membrane, avoiding contamination from cytoplasmic signals (Axelrod *et al.* 1983). The spectral properties of Cyan Fluorescent Protein (CFP) and Yellow Fluorescent Protein (YFP) are well matched for measuring FRET and these fluorophores can be genetically engineered into any protein (Heim & Tsien, 1996). We constructed a series of CFP and YFP fusion proteins (including Kir3 channels, Gαo subunits, GABA$_B$ receptors and RGS4 proteins) for FRET analysis of possible associations within this signalling pathway. Proteins that bring the CFP/YFP fluorophores within 100 Å of each other would be expected to generate a FRET signal.

Methods

Molecular biology

CFP and YFP (we use the terms 'CFP' and 'YFP' for enhanced CFP (eCFP) and enhanced YFP (eYFP), respectively) fusion proteins were constructed as follows. For all C-terminal fusions proteins, the stop codon was eliminated by PCR mutagenesis. For Kir3.2a–YFP and Kir3.2a–CFP, Kir3.2a (Lesage *et al.* 1994) cDNA was subcloned by PCR into Xho1/HindIII sites of pEYFP-N1 or pECFP-N1 (BD Biosciences Clontech, Mountain View, CA, USA). CFP–Kir3.4 and Kir3.1–YFP cDNAs were provided by Riven *et al.* (2003). For Kir2.1*–YFP, the GYG sequence in the pore of Kir2.1 (Kubo *et al.* 1993) was mutated to AAA (denoted by *) using overlapping PCR and subcloned into the Xho1 and BamH1 of pEYFP-N1. For GABA$_B$ R1/R2–YFP and R1/R2–CFP, GABA$_B$ R1 and R2 cDNAs were subcloned by PCR into EcoR1/Age1 sites of pEYFP-N1/pECFP-N1. For RGS4–CFP, RGS4 was amplified using RT-PCR with rat brain RNA and subcloned into XhoI/AgeI site of pECFP-N1. For m1–YFP muscarinic receptor, human m1 receptor was subcloned by PCR into XhoI/HindIII of pEYFP-N1. For rat Gαo fusions, AgeI site was created after E94, M114 and I261 in Gαo–pcDNA3.1$^+$. The eCFP was amplified from pECFP-N1 by PCR with an amino acid linker flanking the eCFP (TGSGGGGSTGGGGS–CFP–GGGGSQGGGGSAG) and spliced into the AgeI site. C351 was mutated to G to make Gαo resistant to Ptx inactivation (Gαo*) (Mutneja *et al.* 2005). We did not observe a significant difference in FRET measurements between the wild-type and Ptx-insensitive versions of CFP-tagged Gαo and therefore pooled these data. For Rho-pYC, the C-terminal prenylation site of Rho (RQKKRRGCLLL) was added to the C-terminal domain of a YFP–CFP fusion (Mayr *et al.* 2001). In RGS4 experiments, Gαo, Gβ1 and Gγ2 cDNA were coexpressed with RGS4–CFP. All constructs were confirmed by DNA sequencing.

Tissue culture and transfections

For most experiments, HEK293T [obtained from America Type Culture Collection (ATCC)] cells were used with the objective of obtaining high expression of signalling proteins. HEK293T is a highly transfectable derivative of the HEK293 that contains the temperature sensitive gene for SV40 T-antigen. We also examined expression of cDNA in HEK293 cells and observed qualitatively similar results. Data was therefore pooled between HEK293T and HEK293 cells, which we collectively refer to as 'HEK293' throughout the paper. HEK293 cells were cultured under sterile conditions in DMEM supplemented with fetal bovine serum (10%), glutamine (2 mM) and penicillin (50 units/ml), streptomycin (50 μg/ml; GIBCO, Invitrogen Corp) in a humidified 37°C incubator with 95% air and 5% CO_2. For FRET experiments, cells were seeded into six-well plates (Corning, Inc.) 3 days prior to experiment. Cells (~50% confluent) were transiently transfected 2 days prior to experiment using the calcium phosphate technique. Briefly, cDNA (0.4–0.8 μg well^{-1}) was mixed in sterile deionized water with 0.25 M $CaCl_2$, then combined 1 : 1 with Hepes-buffered saline containing (mM): NaCl 280, KCl 10, Na_2HPO_4 1.5, glucose 12 and Hepes 50 (pH adjusted to 6.9 with ~1 N NaOH), to yield a final volume of 10% of the total well volume. The mixture was added to cells in six-well plates and incubated for 24 h at 37°C. The day before experiments, cells were reseeded onto 35 mm glass-bottomed cell culture dishes (containing a collagen-coated, #1 thickness, 14 mm glass coverslip; MatTeck Corp. Ashland, MA, USA). For imaging, cells were bathed in Hanks' balanced salt solution (Gibco Invitrogen Corp., Carlsbad, CA, USA; 14065–056) in the absence or presence of baclofen (Sigma-Aldrich, Inc., St. Louis, MO, USA) or CPG5546 (30 μM; Tocris Bioscience, Bristol, UK) for 3–25 min. Cells were approximately 80% confluent on the day of experiment. For Ptx treatment, Ptx (250 ng ml^{-1}) was added to each dish 4–24 h prior to experiment.

For electrophysiological recordings, HEK293 or HEK293T cells were plated onto 12 mm glass coverslips (Warner Instruments) coated with poly-D-lysine (20 μg ml^{-1}; Sigma-Aldrich, Inc) and collagen (100 μg ml^{-1}; BD Biosciences) in 24-well plates. Cells were transiently transfected using the calcium phosphate method as above except that the DNA mixture (0.05–0.1 μg well^{-1}) was added to cells in 24-well plates and incubated for 16–32 h at 37°C, and cells were not reseeded.

Electrophysiology

Whole-cell, patch-clamp technique (Hamill *et al.* 1981) was used to record macroscopic currents from HEK293 cells. Borosilicate glass (Warner; P6165T) electrodes had resistances of 1–3 MΩ and were coated with Sylgard to reduce capacitance. Membrane currents were recorded with an Axopatch 200B (Axon Instruments-Molecular Devices Corp., Sunnyvale, USA) amplifier, adjusted electronically for cell capacitance and series resistance (80–100%), filtered at 2 kHz with an 8 pole Bessel filter, digitized at 5 kHz with a Digidata 1320 interface (Axon Instruments-Molecular Devices Corp., Sunnyvale, USA) and stored on a laboratory computer. The intracellular pipette solution contained (mM): KCl 130, NaCl 20, EGTA 5, K_2ATP 2.56, $MgCl_2$ 5.46 and Hepes 10; pH was adjusted to 7.2 with ~14 mM KOH. There was ~140 mM K^+, 1.5 mM free Mg^{2+} and 2 mM MgATP in the intracellular solution. Li_3-GTP (300 μM; Sigma) was added fresh to the intracellular pipette solution. The external bath solution (20K) contained (mM): NaCl 140, KCl 20, $CaCl_2$ 0.5, $MgCl_2$ 2 and Hepes 10 (pH 7.2); osmolarity 310–330 mosmol l^{-1}. For measurement of leakage current, 20 mM KCl was replaced by 20 mM NaCl to give 160 mM extracellular Na^+ (160Na). Currents were elicited with one of two protocols: a 200 ms voltage ramp from −100 to +50 mV delivered at 0.33 Hz, or continuous current recording at −80 mV. Agonist-independent current (basal) was determined by subtracting the current in 160Na from that in 20K. For ethanol activation, 100% ethanol was added directly to the 20K solution to give 200 mM ethanol (density, 0.7893 g ml^{-1}). $GABA_B$ receptors were activated with 100–300 μM (±)-baclofen (Sigma-Aldrich, Inc). Current–voltage relations were not corrected for the junction potential of ~4 mV, estimated using the Junction Potential Calculator (Axon Instruments - Molecular Devices Corp.). Activation and deactivation time constants were measured by fitting the current traces with a single exponential.

TIRF microscopy and FRET measurements

Through-the-objective TIRF microscopy is achieved when collimated laser light is offset to illuminate the back focal plane of the objective, which causes the laser light to arrive at the coverslip at an angle (Fig. 3*A*). When this angle is greater than the critical angle (θ), an evanescent wave of excitation light is produced at the interface between two media having different refractive indices, the glass coverslip and the media or cell membrane (Axelrod *et al.* 1983). The intensity of this evanescent wave falls off exponentially with distance above the interface, allowing selective imaging within ~100 nm of the glass–medium interface (i.e. plasma membrane and submembrane regions). For TIRF microscopy, we used a Nikon TE2000 microscope, a 60× oil-immersion TIRF objective (Nikon; 1.45 NA), and either a tunable krypton–argon laser tuned to 514 nm (Melles Griot; model, 643-AP-A01) or a solid state DPSS 442 nm laser (Melles Griot; model, 85 BTL 010). The light from a Polychrome IV monochromator (Till Photonics) was also combined with the laser into a single condenser at 50% intensity for both laser and monochromator. The Nikon filter cube contained a polychroic mirror with reflection bands at 440 and 510 nm and band-passes at 475/30 and 560/60 nm (z442/514rpc; Chroma Technology Corp., Bockingham, VT, USA). No excitation filters were used. CFP and YFP emission filters (470/30 for CFP_{Em} and 535/50 nm for YFP_{Em}, respectively) were placed in a filter wheel (Sutter Instruments) and controlled by a Lambda 10–2 controller (Sutter Instruments). Images 16 bit were acquired with a Till 12.5 MHz Imago CCD camera (Till Photonics). The camera, laser shutters and filter wheel were electronically controlled by TILLvisION 4.0 software. Images were analysed using TILLvisION 4.0 software and NIH ImageJ software (FRETcalcv1 plugin).

FRET efficiency (%FRET) was measured using the acceptor photobleaching (APB) method (Zal & Gascoigne, 2004; Takanishi *et al.* 2006; Vogel *et al.* 2006). One advantage of the APB method is that only the change in CFP fluorescence is used to calculate the %FRET, making it possible to compare the measured FRET among different studies (Vogel *et al.* 2006). In contrast, measuring the YFP emission with CFP excitation (three-cube method, or sensitized emission), requires correction for bleed-through and cross-talk fluorescence (Takanishi *et al.* 2006; Vogel *et al.* 2006). The following APB protocol was used for FRET measurements. We used the 442 laser to locate transfected cells and focus the image for subsequent acquisition. This procedure led to some unavoidable direct photobleaching of CFP, which recovered over time (2–3% increase). We typically waited 60 s to allow for CFP recovery before collecting data. We observed a small (0–5%) increase in CFP fluorescence in controls cells expressing only CFP. One potential disadvantage of APB is the movement of fluorophores during the bleaching period. This is especially important with TIRF microscopy, where fluorophores located cytoplasmically (therefore not excited) could move to the plasma membrane during the bleaching time (and therefore subsequently be excited). We examined this possibility by fixing the cells in paraformaldehyde, and then measuring the CFP fluorescence before and after APB in cells expressing only CFP. Under these conditions, we measured a 0–2% increase in CFP fluorescence (data not shown) that is probably due to recovery of photobleached CFP. The additional increase observed in live cells expressing only CFP probably represents equilibration of bleached membrane fluorophores and unbleached cytoplasmic fluorophores; we cannot exclude a small contribution by newly inserted membrane proteins, or a change in the cell footprint.

Images (16 bit) were acquired for CFP fluorescence (400 ms exposure, 2×2 binning – 442 nm laser, CFP_{Em} filter), FRET fluorescence (400 ms exposure, 2×2 binning – 442 nm laser, YFP_{Em} filter) and YFP fluorescence (100 ms exposure, 2×2 binning – 514 nm laser, YFP_{Em} filter) before and after photobleaching (60–90 s) with the 514 nm laser and monochromator tuned to 514 ± 8 nm. The combination of laser and monochromator consistently produced ~20% more bleaching of YFP (~92% total bleaching), increasing the FRET efficiency (see online Supplemental Material Fig. S1). Furthermore, because proteins are in dynamic equilibrium between plasma membrane and cytoplasm, it was advantageous to photobleach cytoplasmic, as well as membrane localized acceptor fluorophores. Measuring CFP only at the membrane ensures that the FRET signal originates only from membrane fluorophores. %FRET was calculated as the percentage increase in CFP emission after photobleaching YFP (eqn (1)):

$$\%\mathrm{FRET} = 100 \times (\mathrm{CFP}_{\mathrm{Em\text{-}post}} - \mathrm{CFP}_{\mathrm{Em\text{-}pre}})/\mathrm{CFP}_{\mathrm{Em\text{-}post}} \quad (1)$$

where $CFP_{Em\text{-}post}$ is CFP emission after photobleaching YFP, and $CFP_{Em\text{-}pre}$ is CFP emission before photobleaching YFP. The %FRET was calculated by drawing regions of interest (ROI) around the cell and subtracting background for each image. We also measured the FRET pixel-by-pixel with two CFP images ($CFP_{Em\text{-}post}$ and $CFP_{Em\text{-}pre}$) using NIH Image J and plugin FRETcalcv1 software, using the following parameters: bleach threshold, 50%; %FRET threshold, −50%; sub-ROI size, 4; donor threshold 4; acceptor threshold, 4. %FRET was comparable using the two methods. 16 bit images were converted to 8 bit for Image J. Images shown in the on-line figures are coloured using Cyan Hot and Yellow Hot look up tables (LUTs) (Image J). CFP and YFP image pairs were scaled to the same pixel range for comparison before and after photobleaching; note that maximal pixel scaling is different across different pair images.

cAMP assay

HEK293 cells were seeded into 48-well plates and transiently transfected 24 h later (using the calcium phosphate method) with cDNA encoding $GABA_B$ R1 and R2 subunits ($0.25\ \mu g\ well^{-1}$), together with either empty plasmid (pcDNA3), Gαo, Gαo* or Gαo*-94–CFP ($0.05\ \mu g\ well^{-1}$). Cells were treated with Ptx ($250\ ng\ ml^{-1}$) the day after transfection, and the cAMP assay performed in triplicate 2 days after transfection. For the cAMP assay, cells were washed in fresh medium, and treated with 3-isobutyl-1-methylxanthine (IBMX) (0.1 μM; 15 min) to block phosphodiesterases, and then treated with forskolin (5 μM; 10 min) to stimulate adenylyl cyclase, in the absence or presence of baclofen (100 μM; 10 min). To rapidly stop the reaction, the entire plate was inverted to remove the liquid and 95% ethanol–0.1 N HCl ($200\ \mu l\ well^{-1}$) was added rapidly to each well. Plates were placed in a −20°C freezer for 30 min. The contents of each well was transferred to an Eppendorf tube, and placed in a vacuum concentrator (Speedvac, Savant) to dry completely. cAMP concentrations were measured using a radioimmunoassay kit, according to the manufacturer's instructions (Biomedical Technologies, BT-300). The assay is based on competitive binding of cAMP in the sample with iodinated cAMP (cAMP-^{125}I) for a highly specific cAMP antibody. Samples were counted in a gamma counter (Apex Automatic; Micromedic Systems) and normalized to forskolin-stimulated data.

Analysis

All values are reported as mean ± S.E.M. Statistical significance was assessed using one-way ANOVA followed by *post hoc* test (Bonferroni), using a significance level of $P < 0.05$ (SigmaStat 3.0).

Results

Function of CFP/YFP-tagged proteins

We showed previously that Gαo interacted directly with Kir3.2a, suggesting that Kir3 channels exist in a signalling complex that contains the GPCR, G protein and Kir3 channel (Clancy *et al.* 2005). To investigate potential protein–protein interactions in living cells, we measured FRET in transiently transfected HEK293 cells using TIRF microscopy. TIRF microscopy enables fluorescence excitation only near the interface between the glass coverslip and the aqueous solution bathing the cells, thereby allowing selective visualization of plasma membrane fluorophores without contamination from fluorophores in the cytoplasm (Axelrod *et al.* 1983). CFP or YFP were fused to the C-terminal domain of $GABA_B$ receptor R1 or R2 subunits, to the N- and C-terminal domains of Kir3.1, Kir3.2a and Kir3.4 channels, and to the C-terminal domain of RGS4. The Kir3.1–YFP and CFP–Kir3.4 constructs were tested previously and shown to undergo FRET (Riven *et al.* 2003). Introduction of CFP into Gα was complicated because the N-terminal domain of Gα is required for anchoring to the plasma membrane and the C-terminal domain is essential for coupling to the GPCR (Wall *et al.* 1995). We therefore inserted CFP into three different loops of Gαo (Fig. 1*A*). Two were located in the helical domain; CFP was inserted after E94 in the loop connecting αA and αB helices, similar to yeast Gα (Janetopoulos *et al.* 2001), and after M114 (loop connecting αB–αC). A third CFP was inserted after I261, just following switch III (between α3 and β5) (Wall *et al.* 1995).

We first investigated the function of the CFP-tagged Gαo by examining the functional coupling of $GABA_B$ receptors to Kir3.2a channels expressed in HEK293 cells. To study the function of ectopically expressed Gαo in the absence of signalling through endogenous Gα, a C-terminal cysteine was mutated thereby rendering the Gαo protein insensitive to Ptx (Avigan *et al.* 1992). Figure 1 shows an example of whole-cell current responses in HEK293 cells pretreated with Ptx (250 ng ml^{-1}; 4 h) to uncouple endogenous G proteins from the $GABA_B$ receptor. Ptx-treated HEK293 cells transfected with wild-type Gαo showed no baclofen-activated Kir3 current, but retained an ethanol-activated Kir3 current, which is G protein independent (Kobayashi *et al.* 1999; Zhou *et al.* 2001). By contrast, HEK293 cells transfected with Gαo*-94–CFP showed robust rescue of the baclofen responses. The basal, ethanol-activated and baclofen-activated Kir3 currents were measured in cells transfected with the different Gαo constructs. Gαo*, Gαo*-94–CFP and Gαo*-114–CFP each rescued baclofen-activated currents to a similar extent in Ptx-treated cells (Fig. 1*D*), indicating that the CFP did not interfere with G protein coupling to Kir3 channel. In Ptx-treated cells, stimulation of Gαo*-94–CFP inhibited forskolin-stimulated cAMP accumulation to a similar extent as Gαo*. The normalized values were 1.15 ± 0.05 ($n = 3$) for pcDNA3.1 vector, 0.99 ± 0.12 ($n = 3$) for wild-type Gαo, 0.22 ± 0.04 ($n = 3$) for Gαo*, and 0.25 ± 0.07 ($n = 3$) for Gαo*-94–CFP (see Methods for details). Gαo-261–CFP, on the other hand, did not appear to couple to Kir3 channels, suggesting the placement of the CFP in this construct interfered with its function (data not shown). We then examined the G protein coupling between YFP-tagged receptors and CFP-tagged channels (Fig. 2*A* and *B*). Coexpression of $GABA_B$ R1–YFP or $GABA_B$ R2–YFP with CFP-tagged channels (Kir3.2a–CFP or CFP–Kir3.4/Kir3.1) resulted in baclofen-induced currents indistinguishable from control (Fig. 2*A* and *B*), suggesting the fluorophores do not demonstrably interfere with the signalling of the proteins. We also studied the ability of RGS4–CFP to modulate Kir3 channel activation. RGS4 accelerates the GTPase activity of Gαo/i G proteins, leading to faster activation and deactivation rates (Doupnik *et al.* 1997). Co-expression of RGS4–CFP with the m2 muscarinic receptor and Kir3.2a channels resulted in carbachol-activated currents that activate and deactivate more rapidly (Fig. 2*C* and *D*).

FRET measured with CFP/YFP-tagged proteins under TIRF microscopy

TIRF microscopy enables the study of fluorescent proteins at a distance of ∼100 nm above the glass coverslip, which includes the plasma membrane and submembrane regions (Fig. 3*A*). To illustrate this, we examined the difference between epifluorescence and TIRF microscopy with cells transfected with Gαo-94–CFP. Figure 3*A* shows CCD images of the same cell collected using either epifluorescence or TIRF illumination (excited at 442 nm and collected using the CFP_{Em} filter). Notice that the surface proteins are readily visible in the TIRF image. We also examined FRET with a construct intrinsically designed to produce basal FRET at the plasma membrane – YFP was fused directly to CFP and anchored to the lipids via a Rho-lipid binding motif (Rho-pYC). Using eqn (1), we calculated the FRET efficiency for Rho-pYC to be 28.0% ± 2.0% ($n = 13$) under TIRF microscopy (see Methods for details).

We next examined possible FRET between Gαo-114–CFP and either $GABA_B$ R1–YFP, $GABA_B$ R2–YFP or Kir3.2a–YFP (Fig. 3*B–E*, see online Supplemental Material Fig. S2). For all experiments using tagged $GABA_B$ receptors, a YFP-labelled subunit was always coexpressed with the untagged partner subunit to form functional heterodimeric receptors (Kaupmann *et al.* 1998; White *et al.* 1998). For controls, CFP-tagged proteins were coexpressed with untagged protein ('no YFP') (Fig. 3*D*, Table 1). Photobleaching of YFP consistently reduced YFP intensity by ∼90% (Fig. 3*B* and *C*, lower panels). An increase (0–5% increase) in CFP following YFP photobleaching was observed in most negative control experiments (i.e. CFP alone). A similar small increase in CFP fluorescence was observed for non-interacting CFP/YFP-tagged protein pairs, following photobleaching

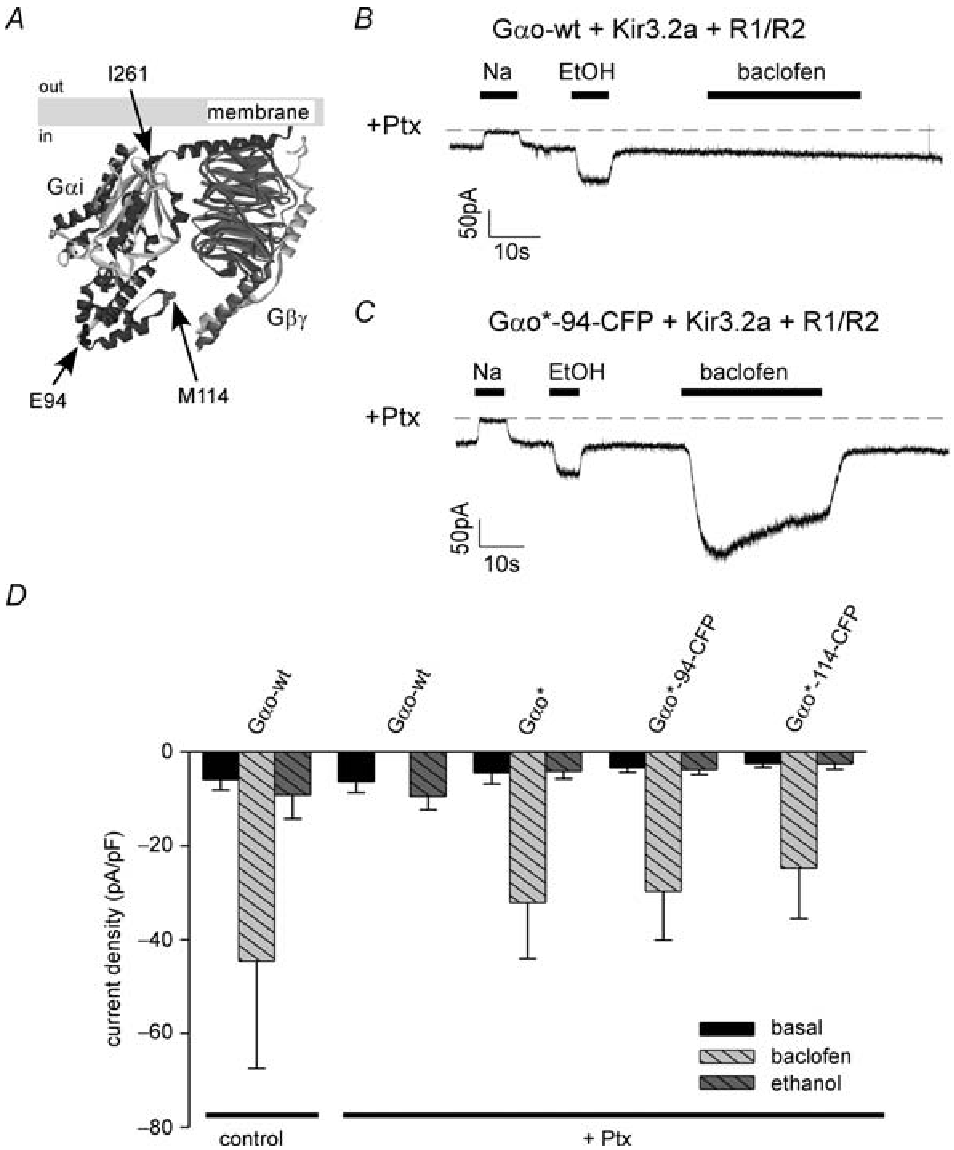

Figure 1. Gαo–CFP G proteins functionally couple to Kir3 channels in HEK293 cells
A, three-dimensional structure of Gα G protein showing CFP insertion sites. Position of CFP is indicated by the arrows in the equivalent region in the Gαi structure [protein data bank (PDB):1GOT]. The $G\beta\gamma$ dimer is also shown. *B–D*, Gαo*-94–CFP G proteins functionally couple to $GABA_B$ receptors. HEK293 cells were transfected with $GABA_B$ R1 or R2 subunits, Kir3.2a and either a pertussis toxin (Ptx)-sensitive Gαo control (Gαo-wt) or a Ptx-insensitive Gαo (Gαo*, Gαo*-94–CFP, or Gαo*-114–CFP). Cells were pretreated with Ptx (except for 'control' in *D*) and whole-cell electrophysiology was used to measure basal, $GABA_B$ receptor-induced, and ethanol-induced currents for Kir3 channels. *B*, Ptx treatment abolishes activation of Kir3.2a by $GABA_B$ receptors in cells expressing wild-type Gαo. Whole-cell current was measured at −80 mV in the presence of 20 mM external K^+. Ethanol-activated current confirms expression of Kir3.2a channels. Dashed line indicates zero current level. *C*, expression of Gαo*-94–CFP rescues $GABA_B$ receptor activation of Kir3.2a in Ptx-treated cells. *D*, bar graph shows mean (± S.E.M.) basal, ethanol-induced and baclofen-induced current densities for cells expressing the indicated constructs (n = 4–5).

YFP (see Table 1). The increase in CFP fluorescence may represent a small fraction of CFP molecules that resensitize and/or move into the evanescent wave during the bleaching protocol (see Methods). Controls were therefore included in every FRET experiment. CFP$_{Em}$ fluorescence clearly increased following APB for Gαo-114–CFP/R1–YFP pair compared with Gαo-114–CFP/Kir3.2a–YFP pair (Fig. 3*B* and *C*, upper panels; see online Supplemental Material Fig. S2). To illustrate this, a histogram of FRET efficiency calculated pixel-by-pixel was compiled, demonstrating a 10–15% increase for R1 and Gαo and −5 to +5% change for Kir3.2a and Gαo (Fig. 3*B* and *C*). The mean %FRET measured over several cells was significantly higher for cells coexpressing R1–YFP or R2–YFP and Gαo-114–CFP (Fig. 3*D*). We also examined possible FRET between Gαo-94–CFP and R1–YFP, R2–YFP or Kir3.2a–YFP. Like Gαo-114–CFP, Gαo-94–CFP showed statistically significant FRET with the GABA$_B$ receptor but not with the channel (Fig. 3*E*). In addition, no significant FRET was observed between the Gαo constructs and either Kir3.1, Kir3.2a or Kir3.4 channels tagged on the N- or C- terminal domain (data not shown). We conclude from these experiments that some Gαo subunits are situated near GABA$_B$ receptors to produce FRET. By contrast, Gαo and Kir3 channels did not show any FRET though these two proteins are presumed to be close. One possible reason for the lack of FRET could be that insertion of fluorophore disrupted the signalling of GαCFP. However, CFP-tagged Gαo subunits can couple to GABA$_B$ receptors and Kir3 channels (Fig. 1). Alternatively, the lack of FRET could indicate that the fluorophore is located in a position unfavourable for FRET with the channel (see Discussion).

We next examined possible FRET between the channel and receptor. HEK293 cells were transfected with Kir3.2a–CFP and YFP-tagged GABA$_B$ R2 or R1 subunits (Fig. 4, see online Supplemental Material Fig. S3). Figure 4*A* shows CFP$_{Em}$ images collected before and after photobleaching from a cell transfected with Kir3.2a–CFP,

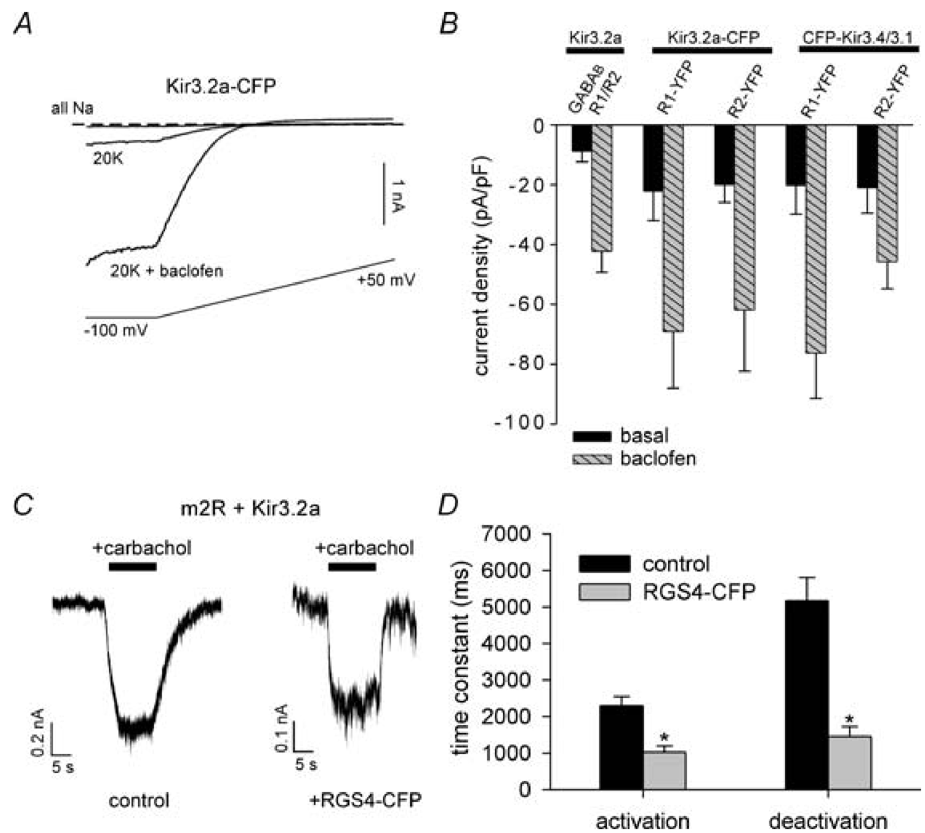

Figure 2. YFP- and CFP-tagged GABA$_B$ receptors and RGS4 protein functionally couple with Kir3 channels
A, basal and baclofen-induced currents elicited by voltage ramps from −100 to +50 mV in a HEK293 cell expressing Kir3.2a–CFP and GABA$_B$ R1 and R2 receptors are shown. Dashed line indicates zero current level. *B*, mean basal and baclofen-induced current densities in cells expressing Kir3.2a–CFP or CFP–Kir3.4/Kir3.1, together with YFP-tagged and untagged GABA$_B$ R1/R2 subunits as indicated. In this and all subsequent experiments using YFP-tagged GABA$_B$ receptor subunits, the untagged partner subunit was always coexpressed to allow formation of a functional GABA$_B$ receptor heterodimer; data are labelled by the subunit bearing the YFP label (n = 6–10). *C*, current traces recorded at −100 mV from HEK293 transfected with Kir3.2a and m2 muscarinic receptors in the absence or presence of coexpressed RGS4–CFP. Note the faster activation and deactivation rates for RGS4–CFP. *D*, bar graph shows mean data for activation and deactivation time constants (n = 6–7).

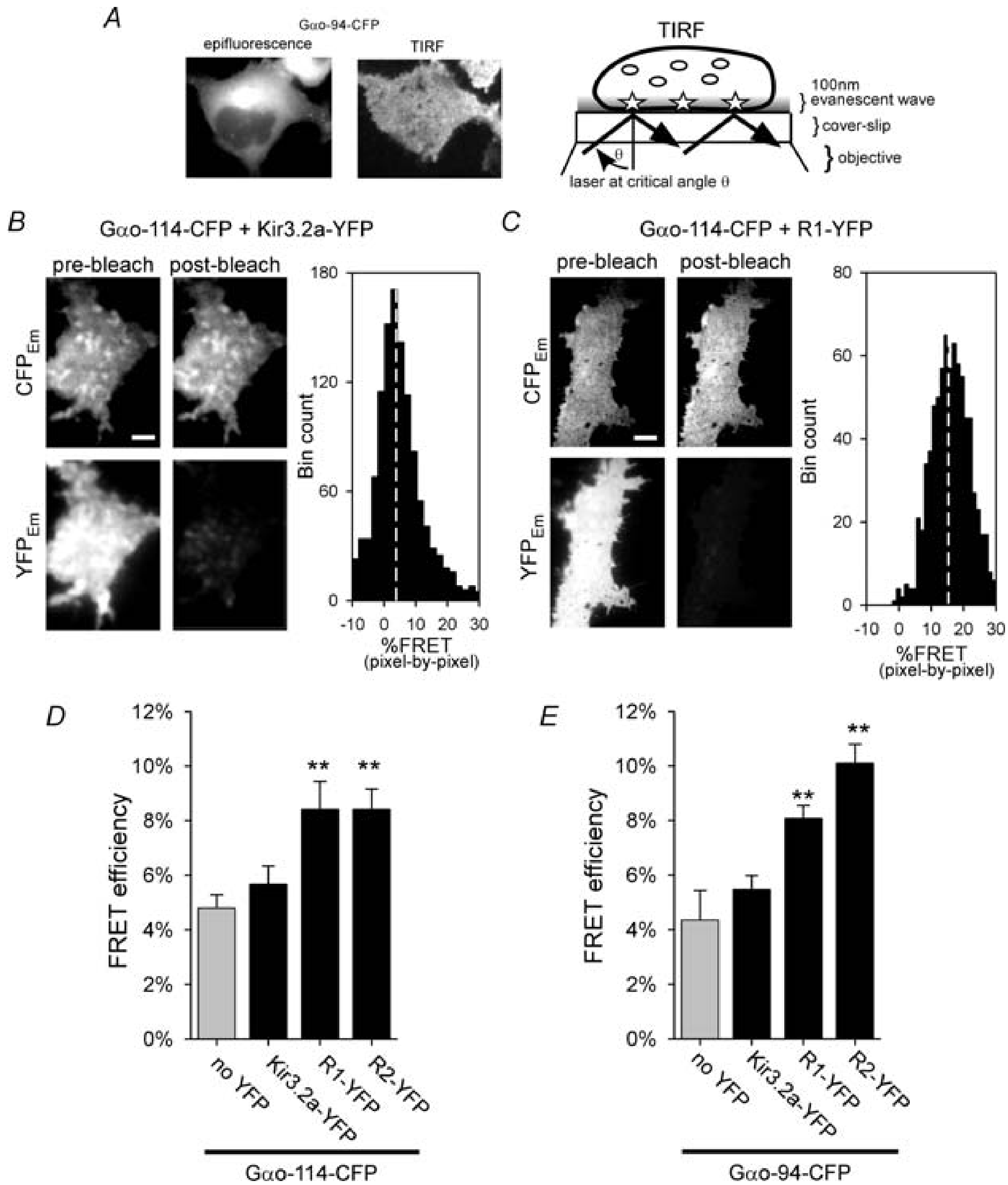

Figure 3. Using TIRF microscopy, FRET is detected between tagged Gαo G proteins and GABA$_B$ receptors, but not between Gαo G proteins and Kir3 channels

A, TIRF allows selective excitation of fluorophores at plasma membrane and submembrane regions near the coverslip–cell interface. Conventional epifluorescence microcopy (left panel) and TIRF microscopy (right panel) images of the same HEK293 cell transfected with Gαo-94–CFP cDNA. Schematic shows side-view of cell and depth of fluorescence measurement under TIRF (not drawn to scale). With through-the-objective TIRF microscopy, an evanescent wave of excitation light is achieved when collimated laser light arrives at the coverslip at an angle greater than the critical angle (θ) – the light falls off exponentially with distance, allowing selective imaging of tissue within a few 100 nm of the glass–medium interface (Axelrod *et al.* 1983). All images and data were acquired using TIRF microscopy. CFP and YFP images were adjusted so that the same pixel range was used before and after photobleaching (note that maximal pixel intensities are different for CFP and YFP). *B* and *C*, images of single cells transfected with Gαo-114–CFP and either Kir3.2a–YFP (*B*) or GABA$_B$ R1–YFP (*C*). Scale bar is 10 μm. *B*, cell expressing Gαo-114–CFP with Kir3.2a–YFP did not exhibit a change in CFP fluorescence following photobleaching of YFP. Note the marked decrease in YFP emission after photobleaching of YFP. FRET efficiency (%FRET) was determined using acceptor photobleaching method (eqn (1)). Histogram shows the distribution of %FRET measured pixel-by-pixel. The peak of distribution is close to 5% for Gαo-114/Kir3.2a. *C*, cell expressing Gαo-114–CFP with GABA$_B$ R2–YFP shows a marked increase in CFP emission following photobleaching of YFP. The peak of %FRET distribution is close to 15% for Gαo-114/GABA$_B$ R1. *D* and *E*, mean FRET efficiency calculated for Gαo-114–CFP (*D*) or Gαo-94–CFP (*E*) and either GABA$_B$ R1–YFP, GABA$_B$ R2–YFP or Kir3.2a–YFP. Statistically significant FRET compared to 'no YFP' controls is indicated by double asterisks (see Table 1).

Table 1. FRET measurements

CFP/YFP-tagged proteins		FRET efficiency			One-way ANOVA **Bonferroni test ($P < 0.05$)
		% FRET	S.E.M.	*n*	
Gαo-94–CFP	no YFP-Kir3.2a	4.4	1.1	19	control
	Kir3.2a–YFP	5.5	0.5	38	
	R1–YFP	8.1	0.5	10	**
	R2–YFP	10.1	0.7	10	**
Gαo-114–CFP	no YFP-Kir3.2a	4.8	0.5	33	control
	Kir3.2a–YFP	5.7	0.7	32	
	R1–YFP	8.4	1.0	13	**
	R2–YFP	8.4	0.7	15	**
Kir3.2a–CFP	R1–YFP	10.1	0.7	25	**
	R2–YFP	10.0	0.6	25	**
	no YFP-R1/R2	4.9	0.5	25	control
R1–CFP	R2–YFP	12.2	0.7	29	**
Kir3.2a–CFP	R1–YFP	7.2	0.5	15	**
	R2–YFP	8.7	0.7	15	**
	no YFP-R1/R2	2.8	0.7	15	control
	Kir2.1*–YFP	4.4	0.4	15	
CFP–Kir3.4/3.1	R1–YFP	9.6	0.4	30	**
	R2–YFP	8.4	0.6	29	**
	no YFP-R1/R2	4.9	1.0	30	control
CFP–Kir3.4/3.1	R1–YFP	7.8	0.2	19	**
	R2–YFP	7.0	0.4	19	**
	no YFP-R1/R2	3.1	0.5	19	control
	Kir2.1*–YFP	4.4	0.4	19	
RGS4–CFP	R1–YFP	13.3	0.8	15	**
	R2–YFP	13.0	0.9	14	**
	no YFP-R1/R2	7.1	0.8	15	control
	Kir3.1–YFP	8.0	1.0	10	
	Kir3.2a–YFP	7.3	0.7	15	
Kir3.2–CFP	m1–YFP	6.3	0.6	10	
Rho-pYC	n/a	28.0	2.0	13	n/a

The %FRET values (mean ± S.E.M.) are shown for the different combinations of CFP/YFP tagged proteins expressed in HEK293 cells. %FRET calculated using acceptor photobleaching method (eqn (1)). n/a, not applicable.

$GABA_B$ R2–YFP and $GABA_B$ R1. The CFP_{Em} intensity increases following APB, and statistically significant FRET was detected between Kir3.2a–CFP and either $GABA_B$ R1–YFP or $GABA_B$ R2–YFP compared to control cells (Fig. 4*D*). We examined the dependence of %FRET on the intensity of CFP (Fc) or YFP (Fy). The %FRET was independent of the levels of CFP or YFP expression, consistent with a FRET signal that did not arise from only non-specific collisions (Fig. 4*B* and *C*). The FRET efficiency for Kir3 channel and $GABA_B$ receptor was comparable to that measured for $GABA_B$ R1–CFP and R2–YFP, which are known to dimerize (Fig. 4*D*). As with Kir3.2a–CFP, significant FRET was detected between CFP–Kir3.4 and either $GABA_B$ R1–YFP or $GABA_B$ R2–YFP subunit (Fig. 4*E* and Table 1). Thus both Kir3.2 and Kir3.4 channels are positioned close enough to $GABA_B$ receptors to generate a significant FRET signal.

To further validate FRET detected between receptor and channel, we carried out negative controls by determining whether FRET could be detected between YFP-tagged membrane proteins that were not expected to interact with Kir3.2a. We used YFP-tagged Kir2.1, which is not activated by GPCRs and is not expected to interact with Kir3 channels. A mutant of Kir2.1, in which the GYG pore motif is mutated to AAA to abolish K^+ currents, was used because high expression of wild-type channels was toxic. FRET efficiency for Kir3.2a–CFP and Kir2.1*–YFP (4.4% ± 0.4; $n = 15$) was not significantly different from CFP alone controls. In addition, we examined the possible FRET between m1 muscarinic receptor and Kir3.2a channels; stimulation of m1 receptors (which are Gq coupled) does not activate Kir3 channels. No significant FRET (6.3% ± 0.6%, $n = 10$) was measured in cells coexpressing m1–YFP and Kir3.2–CFP. These findings indicate the FRET measured between the GPCR and Kir3 channel is specific for the Ptx-sensitive signalling pathway.

We next examined whether stimulation of the $GABA_B$ receptors altered the FRET signal between Kir3 channels and $GABA_B$ receptors. Cells were divided into two groups: 'activated' – cells were incubated in baclofen (100–300 μM) for 3–25 min, and 'control' – cells were incubated in $GABA_B$ receptor antagonist CPG5546 (30 μM) for 3–25min. We observed no statistical difference in the %FRET in cells treated with agonist or antagonist (Fig. 5*A* and *B*). Therefore, the association between $GABA_B$ receptors and Kir3 channels appears to exist in the absence of G protein activation, and persists during receptor activation. In HEK293 cells coexpressing $GABA_B$ receptors and Kir3.2a channels, the baclofen-induced current desensitizes by 60–70% over 2–3 min (Mutneja *et al.* 2005). Thus, many of the activated receptors have desensitized with the agonist stimulation for 3–25 min, suggesting that the FRET measured may reflect receptors in activated and desensitized states (see Discussion).

Finally, we examined the possible association of RGS4 with the Kir3 channel and/or receptor using FRET measurements. RGS4 modulates Kir3 channel activation and deactivation rates (Doupnik *et al.* 1997), suggesting that RGS4 may be localized with the signalling complex. We studied the possible FRET between RGS4–CFP and $GABA_B$ R1–YFP or R2–YFP, and RGS4–CFP and Kir3.1–YFP or Kir3.2a–YFP (Fig. 6, see online Supplemental Material Fig. S4). Figure 6*A* shows CFP_{Em} and YFP_{Em} images collected before and after APB in cells

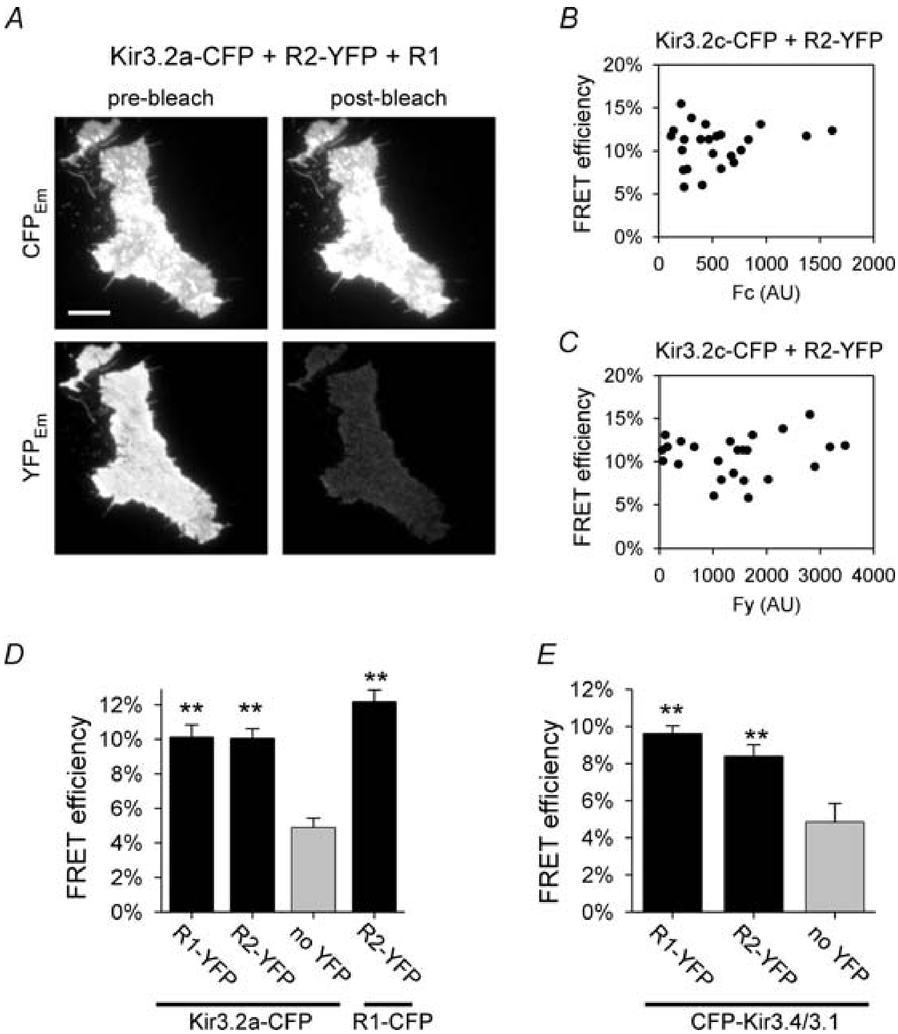

Figure 4. FRET occurs between Kir3 channels and $GABA_B$ receptors
A, HEK293 cells were transfected with Kir3.2a–CFP, $GABA_B$ R2–YFP and R1 cDNA. Images show CFP emission before (left) and after (right) photobleaching of YFP. Scale bar is 10 μm. CFP and YFP images were adjusted so that the same pixel range was used before and after photobleaching (note that maximal pixel intensities are different for CFP and YFP). *B* and *C*, %FRET is plotted for individual cells as a function of CFP intensity (Fc) or YFP intensity (Fy). %FRET was not dependent on the intensities of CFP or YFP. *D*, bar graphs show the mean %FRET. Significant FRET was measured between Kir3.2a–CFP and either R1–YFP or R2–YFP subunit of the $GABA_B$ receptor. For comparison, ~12% FRET efficiency was measured between $GABA_B$ R1–CFP and $GABA_B$ R2–YFP (see Table 1). *E*, summary of %FRET for CFP–Kir3.4/Kir3.1 and R1–YFP or R2–YFP. Both Kir3.2 and Kir3.4 channels appear to associate with $GABA_B$ receptors in HEK293 cells.

transfected with RGS4–CFP, $GABA_B$ R2–YFP and $GABA_B$ R1. Note the increase in CFP_{Em} fluorescence following photobleaching of $GABA_B$ R2–YFP. Statistically significant FRET was detected between RGS4–CFP and either $GABA_B$ R1–YFP or $GABA_B$ R2–YFP in numerous cells (Fig. 6*D* and Table 1). As described above, we examined the dependence of the percentage FRET on Fc and Fy. The %FRET was independent of the levels of CFP or YFP expression, suggesting the %FRET signal did not arise from non-specific collisions (Fig. 6*B* and *C*). No FRET was detected between RGS4–CFP and either Kir3.1–YFP or Kir3.2a–YFP (Fig. 6*D*).

Discussion

In the current study, we used FRET measurements and live imaging to probe the molecular interactions of proteins within a Kir3 signalling complex, including $GABA_B$ receptors, Gαo G proteins, Kir3 channels and RGS4 proteins. We found that $GABA_B$ receptors and Kir3 channels, as well as $GABA_B$ receptors and RGS4 proteins, move within the 100 Å needed to generate FRET. It is important to note that the fluorophore-tagged proteins used in our study were functional; they could mediate G protein activation and modulation of Kir3 channels via stimulation of $GABA_B$ receptors.

One advantage of using the APB method is the ability to compare the %FRET among different studies. The %FRET (8–13%) in our study compares favourably with ~15% FRET for GPCR and Gα (Nobles *et al.* 2005), ~20% FRET for Kir3.1–YFP and CFP–Kir3.4 channels (Riven *et al.* 2003), and 30% FRET for $GABA_B$ R1 and R2 subunits (Uezono *et al.* 2006). It is interesting that we did not detect FRET between Gαo and Kir3 channels or between RGS4 and Kir3 channels. There are several different scenarios that can result in little or no FRET. First, if the two fluorophores are not close enough (> 100 Å), then there will be no FRET. Second, FRET will not occur if the dipoles of CFP and YFP are perpendicular (even if the two proteins are within 100 Å). This possibility seems unlikely for Gαo because CFP was inserted into two different positions, probably leading to two different orientations of CFP. Third, the insertion of the CFP could interfere with the ability of the tagged protein to directly associate with the channel. However, $GABA_B$ receptor stimulation of Gαo–CFP led to activation of Kir3 channels and RGS4–CFP expression resulted in faster Kir3 channel kinetics. In addition, Gαo–CFP or RGS4–CFP were able to undergo FRET with other YFP-tagged proteins. As we cannot distinguish between these possibilities, our experiments do not provide evidence for or against a direct association between Kir3 channels and either Gαo or RGS4 proteins. It is interesting that Riven *et al.* (2006) recently used FRET measurements to provide evidence that the G$\alpha\beta\gamma$ heterotrimer associates with Kir3 channels in the resting state.

For one model of $GABA_B$ receptor signalling, the R1 subunit is believed to bind ligand while the R2 subunit signals to G proteins (Bettler *et al.* 2004). We found that FRET occurred between Gαo–CFP and both YFP-tagged $GABA_B$

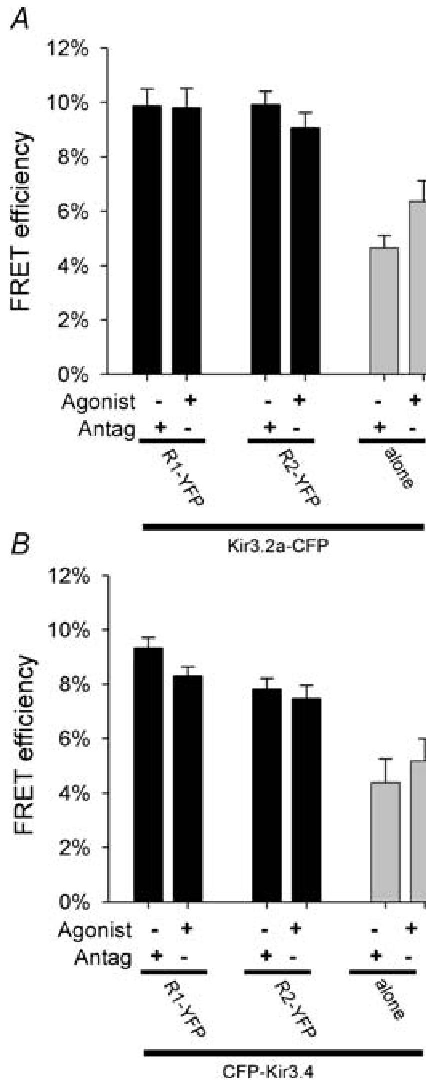

Figure 5. No effect of $GABA_B$ receptor stimulation on FRET between $GABA_B$ receptors and Kir3 channels
Transfected cells were divided into two treatment groups: 'activated' receptors (agonist) and control (antagonist). *A*, FRET efficiency between Kir3.2a–CFP and either $GABA_B$ R1–YFP or $GABA_B$ R2–YFP was not significantly different in cells exposed to $GABA_B$ receptor agonist baclofen (300 μM) for 3–25min from that in cells exposed to $GABA_B$ receptor antagonist CPG5546 (30 μM) for 3–25min. For agonist and antagonist groups, %FRET was 9.8 ± 0.68% *versus* 9.9 ± 0.6% for R1–YFP and 9.1 ± 0.6% *versus* 9.9 ± 0.5% for R2–YFP (n = 25–30). *B*, similarly, FRET between CFP–Kir3.4/3.1 and either $GABA_B$ R1–YFP or R2–YFP was not significantly different between agonist-treated (300 μM baclofen for 3–25min) and antagonist-treated (30 μM CPG5546 for 3–25min). For agonist and antagonist groups, %FRET was 8.3 ± 0.3% *versus* 9.3 ± 0.4% for R1–YFP and 7.5 ± 0.5% *versus* 7.8 ± 0.4% for R2–YFP (n = 26–36).

R1 and R2 receptor subunits. These findings suggest that Gαo–CFP is situated near both R1 and R2 subunits in the resting state. We cannot estimate from our measurements what fraction of receptors and Gαo associate. The FRET signal may represent a fraction of Gαo–CFP that stably associates with R1 and R2, or a time-averaged signal from continuously associating/disassociating receptors and G proteins, or a combination of both. Two recent studies provide evidence that components of the G protein signalling pathway move independently within the membrane. Azpiazu & Gautam (2004) used a FRET-based approach to show that the same pool of G proteins couple consecutively with different receptors, indicating that if a stable complex exists, the Gα G proteins do not (or at least not all of them) form part of it. Similarly, Hein *et al.* (2005) found little evidence for precoupling between the α2a-adrenergic receptor and Gαi G proteins, and suggested a collision coupling as a mechanism for this receptor–G protein pair. In contrast to our study, no basal FRET between receptor and G protein was detected in their study. Gales *et al.* (2005), on the other hand, measured FRET between Gαs and the β2-adrenergic receptor in the absence of receptor stimulation, as did Benians *et al.* (2003) for Gαo with either the α2-adrenergic receptor, m4 muscarinic receptor, A1 adenosine receptor or D2S dopamine receptor. The disparities between the results of these studies underscore the need to study the detailed mechanism of G protein coupling with specific receptors and effectors expressed in their native environment.

In addition to the Gαo–CFP, significant FRET was measured between YFP-tagged $GABA_B$ R1 and R2 subunits and Kir3.2a–CFP or CFP–Kir3.4. The %FRET was similar

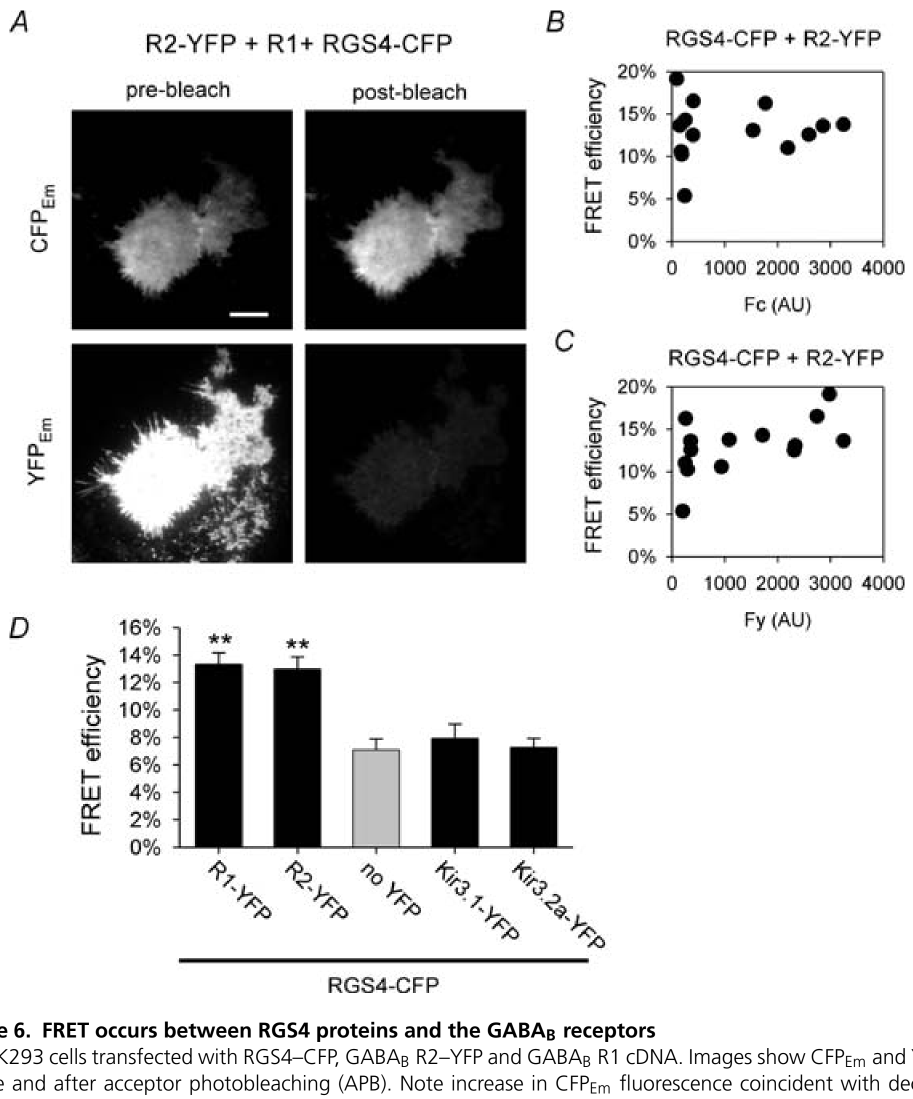

Figure 6. FRET occurs between RGS4 proteins and the $GABA_B$ receptors
A, HEK293 cells transfected with RGS4–CFP, $GABA_B$ R2–YFP and $GABA_B$ R1 cDNA. Images show CFP_{Em} and YFP_{Em} before and after acceptor photobleaching (APB). Note increase in CFP_{Em} fluorescence coincident with decrease in YFP_{Em} following APB. Scale bar is 10 μm. *B* and *C*, FRET efficiency (%FRET) is plotted as a function of CFP intensity (Fc) or YFP intensity (Fy). %FRET was not dependent on the intensities of CFP or YFP. *D*, bar graph shows mean FRET efficiency between RGS4–CFP and R1–YFP, R2–YFP, Kir3.1–YFP/Kir3.2 and Kir3.2a–YFP. Gαβγ was also coexpressed. Significant FRET was detected between RGS4 and $GABA_B$ receptors, but not between RGS4 and Kir3 channels.

to that measured between the R1 and R2 subunits of the $GABA_B$ receptor, which are known to heterodimerize. Discovering that Kir3 associates closely with $GABA_B$ receptors was unexpected. Initially, we hypothesized that G proteins are docked on Kir3 channels in the absence of receptor stimulation (Clancy *et al.* 2005) – the $GABA_B$ receptor would be predicted to be near the Gα G protein but probably too far from Kir3 to generate a FRET signal. Our current FRET data, however, suggest that Kir3 channels associate closely with $GABA_B$ receptors in the absence of receptor activation. Recent biochemical data support this model. Dopamine D2 receptors can coprecipitate with Kir3 channels (Lavine *et al.* 2002). Furthermore, using bioluminescence resonance energy transfer measurements to detect associations, β2-adrenergic receptors were found to be near both Kir3 channels and another effector, adenylyl cyclase (Zamah *et al.* 2002). Together, these studies suggest that precoupling may involve the GPCR, G protein, RGS protein and channel. Additional biochemical studies with natively expressed proteins will help confirm these associations between $GABA_B$ receptors and Kir3 channels. We speculate that a preformed signalling complex may not apply to all G protein signalling pathways. For example, receptor activation of Gαs causes translocation of the Gα subunit from the plasma membrane to the cytoplasm (Thiyagarajan *et al.* 2002). The lipid composition and formation of subcellular compartments may also be important for determining the structure and stability of signalling complexes. $GABA_B$ receptors, Kir3 channels and Gαi G proteins associate with lipid rafts (Becher *et al.* 2001; Oh & Schnitzer, 2001; Koyrakh *et al.* 2005). The formation of specific receptor–channel complexes could be an important requirement for signalling in neurons. For example, $GABA_B$ receptors couple efficiently to Kir3 channels in dendrites of hippocampal neurons (Lüscher *et al.* 1997). Consistent with the view of a Kir3 signalling complex, immunohistochemical studies have demonstrated that $GABA_B$ receptors and Kir3.2 channels are situated physically close in these neurons (Kulik *et al.* 2006) and FRET was detected between Kir3 channels and G protein heterotrimer (Riven *et al.* 2006).

The FRET measured between $GABA_B$ receptors and Kir3 channels did not change significantly upon exposure to agonist. In our experiments, the cells are continuously bathed in baclofen raising the possibility that the receptors have partially or completely desensitized. Although $GABA_B$ receptors do not undergo endocytosis during chronic stimulation, they can exhibit desensitization through a G protein-dependent mechanism (Mutneja *et al.* 2005). Thus, receptors may remain associated (< 100 Å) with Kir3 channels during receptor activation and desensitization. Consistent with this, Lavine *et al.* (2002) reported no change in FRET between β2-adrenergic receptors and Kir3 channels upon agonist stimulation and could coprecipitate D2 receptors with Kir3 channels under basal and activated conditions. Together, these data suggest that these receptor–effector interactions persist during signalling; however, more studies are needed to examine what fraction of receptors stably associate with Kir3 channels in complexes.

Finally, we observed significant FRET between the $GABA_B$ receptor and RGS4 protein. This suggests that RGS protein, acting as a GAP for Gα, is located near to the $GABA_B$ receptor. Consistent with this, Georgoussi *et al.* (2006) demonstrated biochemically that RGS4 can interact directly with both the δ- and μ-opioid receptors. It will be interesting to determine whether RGS4 binds directly to the $GABA_B$ receptor or associates with the receptor via the G protein heterotrimer. Benians *et al.* (2005) did not detect FRET between RGS8 and D2 dopamine receptors, suggesting the interaction could be dependent on the type of RGS and/or receptor subtype. If there is a difference in association of different RGS isoforms with the $GABA_B$ receptor, then this may correlate with their relative GAP activity in signalling pathways involving different receptors (Benians *et al.* 2005).

In summary, we have detected FRET between several proteins within the Kir3 signalling complex. These data argue for a close association (within 100 Å) between $GABA_B$ receptors, Gαo G proteins, RGS4 proteins and Kir3 channels. Although we were unable to detect FRET between Gα and channel, the proximity of receptor and G protein, and receptor and channel, favour a close association between Gα and Kir3 channels. The close association of these proteins is probably important for the rapid and specific activation of Kir3 channels in neuronal, endocrine and cardiac cells.

References

Avigan J, Murtagh JJ Jr, Stevens LA, Angus CW, Moss J & Vaughan M (1992). Pertussis toxin-catalyzed ADP-ribosylation of G_o alpha with mutations at the carboxyl terminus. *Biochemistry* **31**, 7736–7740.

Axelrod D, Thompson NL & Burghardt TP (1983). Total internal inflection fluorescent microscopy. *J Microsc* **129**, 19–28.

Azpiazu I & Gautam N (2004). A fluorescence resonance energy transfer-based sensor indicates that receptor access to a G protein is unrestricted in a living mammalian cell. *J Biol Chem* **279**, 27709–27718.

Becher A, White JH & McIlhinney RA (2001). The gamma-aminobutyric acid receptor B, but not the metabotropic glutamate receptor type-1, associates with lipid rafts in the rat cerebellum. *J Neurochem* **79**, 787–795.

Benians A, Leaney JL, Milligan G & Tinker A (2003). The dynamics of formation and action of the ternary complex revealed in living cells using a G-protein gated K^+ channel as a biosensor. *J Biol Chem* **278**, 10851–10858.

Benians A, Nobles M, Hosny S & Tinker A (2005). Regulators of G-protein signaling form a quaternary complex with the agonist, receptor, and G-protein: a novel explanation for the acceleration of signaling activation kinetics. *J Biol Chem* **280**, 13383–13394.

Bettler B, Kaupmann K, Mosbacher J & Gassmann M (2004). Molecular structure and physiological functions of $GABA_B$ receptors. *Physiol Rev* **84**, 835–867.

Bloch W, Fan Y, Han J, Xue S, Schoneberg T, Ji G, Lu ZJ, Walther M, Fassler R, Hescheler J, Addicks K & Fleischmann BK (2001). Disruption of cytoskeletal integrity impairs Gi-mediated signaling due to displacement of Gi proteins. *J Cell Biol* **154**, 753–761.

Bunemann M, Frank M & Lohse MJ (2003). Gi protein activation in intact cells involves subunit rearrangement rather than dissociation. *Proc Natl Acad Sci U S A* **100**, 16077–16082.

Clancy S, Fowler C, Finley M, Arrabit C, Suen K-F, Berton F, Kozasa T, Casey P & Slesinger PA (2005). Pertussis-toxin-sensitive Gα subunits selectively bind to C-terminal domain of neuronal GIRK channels: evidence for a heterotrimeric G-protein-channel complex. *Mol Cell Neurosci* **28**, 375–389.

Doupnik CA, Davidson N, Lester HA & Kofuji P (1997). RGS proteins reconstitute the rapid rating kinetics of G$\beta\gamma$-activated inwardly rectifying K^+ channels. *Proc Natl Acad Sci U S A* **94**, 10461–10466.

Gales C, Rebois RV, Hogue M, Trieu P, Breit A, Hebert TE & Bouvier M (2005). Real-time monitoring of receptor and G-protein interactions in living cells. *Nat Methods* **2**, 177–184.

Georgoussi Z, Leontiadis L, Mazarakou G, Merkouris M, Hyde K & Hamm H (2006). Selective interactions between G protein subunits and RGS4 with the C-terminal domains of the [mu]- and [delta]-opioid receptors regulate opioid receptor signaling. *Cell Signal* **18**, 771–782.

Hamill OP, Marty A, Neher E, Sakmann B & Sigworth FJ (1981). Improved patch-clamp techniques for high-resolution current recording from cells and cell-free membrane patches. *Pflugers Arch* **391**, 85–100.

Heim R & Tsien RY (1996). Engineering green fluorescent protein for improved brightness, longer wavelengths and fluorescence resonance energy transfer. *Curr Biol* **6**, 178–182.

Hein P, Frank M, Hoffmann C, Lohse MJ & Bunemann M (2005). Dynamics of receptor/G protein coupling in living cells. *EMBO J* **24**, 4106–4114.

Huang CL, Slesinger PA, Casey PJ, Jan YN & Jan LY (1995). Evidence that direct binding of G$\beta\gamma$ to the GIRK1 G protein-gated inwardly rectifying K^+ channel is important for channel activation. *Neuron* **15**, 1133–1143.

Janetopoulos C, Jin T & Devreotes P (2001). Receptor-mediated activation of heterotrimeric G-proteins in living cells. *Science* **291**, 2408–2411.

Jares-Erijman EA & Jovin TM (2003). FRET imaging. *Nat Biotechnol* **21**, 1387–1395.

Kaupmann K, Malitschek B, Schuler V, Heid J, Froestl W, Beck P, Mosbacher J, Bischoff S, Kulik A, Shigemoto R, Karschin A & Bettler B (1998). $GABA_B$-receptor subtypes assemble into functional heterometic complexes. *Nature* **396**, 683–687.

Klein S, Reuveni H & Levitzki A (2000). Signal transduction by a nondissociable heterotrimeric yeast G protein. *Proc Natl Acad Sci U S A* **97**, 3219–3223.

Kobayashi T, Ikeda K, Kojima H, Niki H, Yano R, Yoshiola T & Kumanishi T (1999). Ethanol opens G-protein-activated inwardly rectifying K^+ channels. *Nat Neurosci* **2**, 1091–1097.

Koyrakh L, Lujan R, Colon J, Karschin C, Kurachi Y, Karschin A & Wickman K (2005). Molecular and cellular diversity of neuronal G-protein-gated potassium channels. *J Neurosci* **25**, 11468–11478.

Kubo Y, Baldwin TJ, Jan YN & Jan LY (1993). Primary structure and functional expression of a mouse inward rectifier potassium channel. *Nature* **362**, 127–133.

Kulik A, Vida I, Fukazawa Y, Guetg N, Kasugai Y, Marker CL, Rigato F, Bettler B, Wickman K, Frotscher M & Shigemoto R (2006). Compartment-dependent colocalization of Kir3.2-containing K^+ channels and $GABA_B$ receptors in hippocampal pyramidal cells. *J Neurosci* **26**, 4289–4297.

Kwon G, Axelrod D & Neubig RR (1994). Lateral mobility of tetramethylrhodamine (TMR) labelled G protein α and $\beta\gamma$ subunits in NG 108–15 cells. *Cell Signal* **6**, 663–679.

Lachance M, Ethier N, Wolbring G, Schnetkamp PP & Hebert TE (1999). Stable association of G proteins with beta 2AR is independent of the state of receptor activation. *Cell Signal* **11**, 523–533.

Lavine N, Ethier N, Oak JN, Pei L, Liu F, Trieu P, Rebois RV, Bouvier M, Hebert TE & Van Tol HH (2002). G protein-coupled receptors form stable complexes with inwardly rectifying potassium channels and adenylyl cyclase. *J Biol Chem* **277**, 46010–46019.

Lesage F, Duprat F, Fink M, Guillemare E, Coppola T, Lazdunski M & Hugnot JP (1994). Cloning provides evidence for a family of inward rectifier and G-protein coupled K^+ channels in the brain. *FEBS Lett* **353**, 37–42.

Lüscher C, Jan LY, Stoffel M, Malenka RC & Nicoll RA (1997). G-protein-coupled inwardly rectifying K^+ channels (GIRKs) mediate postsynaptic, but not presynaptic transmitter actions in hippocampal neurons. *Neuron* **19**, 687–695.

Mayr BM, Canettieri G & Montminy MR (2001). Distinct effects of cAMP and mitogenic signals on CREB-binding protein recruitment impart specificity to target gene activation via CREB. *Proc Natl Acad Sci U S A* **98**, 10936–10941.

Mutneja M, Berton F, Suen K-F, Luscher C & Slesinger PA (2005). Endogenous RGS proteins enhance acute desensitization of GABAB receptor-activated GIRK currents in HEK-293T cells. *Pflugers Arch* **450**, 61–73.

Nobles M, Benians A & Tinker A (2005). Heterotrimeric G proteins precouple with G protein-coupled receptors in living cells. *Proc Natl Acad Sci U S A* **102**, 18706–18711.

Oh P & Schnitzer JE (2001). Segregation of heterotrimeric G proteins in cell surface microdomains. G(q) binds caveolin to concentrate in caveolae, whereas G(i) and G(s) target lipid rafts by default. *Mol Biol Cell* **12**, 685–698.

Peleg S, Varon D, Ivanina T, Dessauer CW & Dascal N (2002). Gαi controls the gating of the G protein-activated K^+ channel, GIRK. *Neuron* **33**, 87–99.

Rebois RV, Warner DR & Basi NS (1997). Does subunit dissociation necessarily accompany the activation of all heterotrimeric G proteins? *Cell Signal* **9**, 141–151.

Reuveny E, Slesinger PA, Inglese J, Morales JM, Iniguez-Lluhi JA, Lefkowitz RJ, Bourne HR, Jan YN & Jan LY (1994). Activation of the cloned muscarinic potassium channel by G protein $\beta\gamma$ subunits. *Nature* **370**, 143–146.

Riven I, Iwanir S & Reuveny E (2006). GIRK channel activation involves a local rearrangement of a preformed G protein channel complex. *Neuron* **51**, 561–573.

Riven I, Kalmanzon E, Segev L & Reuveny E (2003). Conformational rearrangements associated with the gating of the G protein-coupled potassium channel revealed by FRET microscopy. *Neuron* **38**, 225–235.

Stanfield PR, Nakajima S & Nakajima Y (2002). Constitutively active and G-protein coupled inward rectifier K^+ channels: Kir2.0 and Kir3.0. *Rev Physiol Biochem Pharmacol* **145**, 47–179.

Takanishi CL, Bykova EA, Cheng W & Zheng J (2006). GFP-based FRET analysis in live cells. *Brain Res* **1091**, 132–139.

Thiyagarajan MM, Bigras E, Van Tol HH, Hebert TE, Evanko DS & Wedegaertner PB (2002). Activation-induced subcellular redistribution of G alpha(s) is dependent upon its unique N-terminus. *Biochemistry* **41**, 9470–9484.

Uezono Y, Kanaide M, Kaibara M, Barzilai R, Dascal N, Sumikawa K & Taniyama K (2006). Coupling of GABAB receptor GABAB2 subunit to G proteins: evidence from Xenopus oocyte and baby hamster kidney cell expression system. *Am J Physiol Cell Physiol* **290**, C200–C207.

Vogel SS, Thaler C & Koushik SV (2006). Fanciful FRET. *Sci STKE* **2006**, re2.

Wall MA, Coleman DE, Lee E, Iniguez-Lluhi JA, Posner BA, Gilman AG & Sprang SR (1995). The structure of the G protein heterotrimer $G_{i\alpha 1}\beta_1\gamma_2$. *Cell* **83**, 1047–1058.

White JH, Wise A, Main MJ, Green A, Fraser NJ, Disney GH, Barnes AA, Emson P, Foord SM & Marshall FH (1998). Heterodimerization is required for the formation of a functional $GABA_B$ receptor. *Nature* **396**, 679–682.

Wickman KD, Iniguez-Lluhl JA, Davenport PA, Taussig R, Krapivinsky GB, Linder ME, Gilman AG & Clapham DE (1994). Recombinant G-protein $\beta\gamma$-subunits activate the muscarinic-gated atrial potassium channel. *Nature* **368**, 255–257.

Zal T & Gascoigne NRJ (2004). Photobleaching-corrected FRET efficiency imaging of live cells. *Biophys J* **86**, 3923–3939.

Zamah AM, Delahunty M, Luttrell LM & Lefkowitz RJ (2002). Protein kinase A-mediated phosphorylation of the beta 2-adrenergic receptor regulates its coupling to Gs and Gi. Demonstration in a reconstituted system. *J Biol Chem* **277**, 31249–31256.

Zhou W, Arrabit C, Choe S & Slesinger PA (2001). Mechanism underlying bupivacaine inhibition of G protein-gated inwardly rectifying K^+ channels. *Proc Natl Acad Sci U S A* **98**, 6482–6487.

Acknowledgements

We thank David Zacharias for his invaluable advice with the FRET microscopy, Eitan Reuveny for providing 1C-YL (Kir3.1–YFP) and 4N-CY (CFP–Kir3.4) cDNAs and advice on TIRF, Andrew Tinker for Gαo cDNA, and Lily Jan for providing $GABA_B$ receptor and RGS4 cDNAs. This work was made possible by financial support from McKnight Endowment for Neuroscience, the Hearst Foundation and the National Institute of Neurological Disorders and Stroke (NIH R01 NS37682).

Author's current address

C. E. Fowler: Department of Neurobiology, Box 2900, Duke University, Durham, NC 27710, USA.

Supplemental material

The online version of this paper can be accessed at:
DOI: 10.1113/jphysiol.2006.123216
http://jp.physoc.org/cgi/content/full/jphysiol.2006.123216/DC1
and contains supplemental material consisting of four figures.

Figure S1. The combination of laser and monochromator to photobleach YFP consistently produced significantly larger decreases in YFP intensity and subsequent increases in CFP emission (%FRET) when compared to laser alone

Figure S2 (colour version of Fig. 3). Using TIRF microscopy, FRET is detected between tagged Gαo G proteins and $GABA_B$ receptors, but not between Gαo G proteins and Kir3 channels

Figure S3 (colour version of Fig. 4). FRET occurs between Kir3 channels and $GABA_B$ receptors

Figure S4 (colour from Fig. 6). FRET occurs between RGS4 proteins and the $GABA_B$ receptors

This material can also be found as part of the full-text HTML version available from http://www.blackwell-synergy.com